Sea Surface Topography and Geostrophic Flow Estimation from Multi-Satellite Altimetry and Shipborne Gravity Data Using Low-pass Filtering and Wavelet Decomposition

G.S. Vergos✉
Department of Geodesy and Surveying, Aristotle University of Thessaloniki, University Box 440, 541 24, Thessaloniki, Greece, Tel: +30 31 0996125, Fax: +30 31 0995948, email: vergos@topo.auth.gr

R.S. Grebenitcharsky, M.G. Sideris
Department of Geomatics Engineering, University of Calgary, 2500 University Drive N.W., Calgary Alberta, T2N 1N4, Canada

Abstract. The possibility of improving the estimation of the quasi-stationary sea surface topography (QSST) and the determination of geostrophic velocities is investigated in an area close to the island of Newfoundland. Multi-satellite (ERS1, GEOSAT) geodetic mission (GM) altimetry and shipborne gravity data are used in an attempt to improve the estimation of the QSST and determine the general circulation pattern in the area under study. Newly estimated local bathymetry models are implemented in the predictions, aiming at providing as smooth residuals as possible before the QSST estimation takes place. The EGM96 geopotential and Dynamic Ocean Topography (DOT) models are used to model the low-frequency part of the gravity field signal and correct the altimetry data for the QSST respectively. The estimation of the QSST using altimetry and shipborne gravity anomalies aims to detect remaining signal at wavelengths shorter than about 2000 km, contrary to what global DOT models imply. Additionally, ocean current velocities, based on the theory of geostrophic flow, are derived to detect the general circulation pattern of the area under study. Blunders in the shipborne data together with high-frequency oceanic phenomena contaminating altimetry sea surface heights can cause the SST estimates to have unreasonably high or small values. To detect and smooth such discrepancies, wavelet decomposition and low-pass filtering are used. The localization property of wavelets is used to detect the distribution of such irregularities, which can be smoothed using a wavelet transform as multiscale differential operator. Smoother SST and geostrophic velocity estimates are derived, showing very good agreement with the circulation pattern of the area.

Keywords. Geostrophic velocities, low-pass filtering, sea surface topography, wavelets.

1 Introduction

During the last two decades satellite altimetry has offered an abundance of measurements of the sea surface, thus improving the determination of the marine gravity field and the marine geoid. These breakthroughs signal a great opportunity for the use of geodetic altimetry-derived products in the estimation of other parameters related to the marine environment. One of these quantities is the QSST, which is of high importance not only for oceanographic studies but for geodetic ones as well, since it is necessary for the reduction of altimetry data from the sea surface to the geoid. Such studies on a *geodetic determination* of the QSST have begun since the advent of altimetry in the early 1980's and the work by Engelis (1983) presented in an elegant way their feasibility (OSU83 QSST model). Consequently, there have been more studies on a global determination of the QSST in terms of spherical harmonics (SH) (Engelis, 1985), while Engelis (1987) presented different solutions based on the expansion of the Levitus SST in terms of SH to degree and order 10, 15 and 20. Knudsen (1992b) used the very simple relation giving the QSST as the difference between an altimetric and a gravimetric geoid to model the QSST in the North Sea and presented a local QSST model accompanied by the geostrophic velocities for the region. Finally, Lemoine et al. (1997) estimated during the adjustment of the EGM96 geopotential model an expansion of the QSST in terms of SH complete to degree and order 20, while Pavlis et al. (1998) used Proudman functions and data from the POCM-4 model to estimate a SST model complete to degree and order 20.

The focus of this paper is to determine local models of the QSST and the geostrophic currents in an area offshore Newfoundland, Canada. This region was selected due to the high ocean dynamics and the presence of well known currents (Labrador Current) and gyres (Gulf Stream), which can provide a reasonable validation of the proposed method. The determination is based on well-known geodetic algorithms and uses purely "geodetic" data, i.e. satellite altimetry geoid heights and shipborne gravity. We consider the simple formula connecting altimetric and gravimetric geoid heights or gravity fields, i.e. that their difference gives the QSST. With this as a starting point, the use of low pass filtering (LPF) and wavelets (WL) are proposed to filter the resulting QSST field and lead to a better approximation of the SST. This filtering operation is necessary to reduce high-frequency oceanic effects contaminating GM altimetry and smooth the differences between the altimetry and shipborne gravity data, due to blunders in the latter.

2 Sea Surface Topography Modeling

To determine the QSST, GM altimetry and shipborne gravity data are used. Depending on which dataset is denser there are two possibilities, i.e., if the altimetry data are denser, then altimetric gravity anomalies are estimated and the difference with the shipborne data gives the so-called *gravity equivalent quasi-stationary sea surface topography* $\Delta g(QSST)$. But, if the shipborne data are denser, then gravimetric geoid heights are estimated and the difference is derived in the geoid domain, thus the QSST (ς_c) is estimated directly. In the present study, the altimetry data were denser, thus that procedure will be described in more detail.

To derive altimetric gravity anomalies the well-known remove-compute-restore method was used. Thus the contribution of a geopotential model and that of the bathymetry were removed from the SSHs, which were corrected for all geophysical effects and instrumental errors in a prior step. The use of the bathymetry intends to provide smoother residuals before the interpolation and/or prediction takes place. An important step in this procedure, usually neglected in related studies, is the reduction of the altimetric observations from the sea surface to the geoid. This is necessary otherwise the estimated quantities will be the mean sea surface (MSS) (if geoid modeling is the objective) or a gravity field that refers to the MSS. This reduction can be performed using a global QSST model and computing the QSST for each SSH observation point.

An additional step refers to crossover adjusting (CA) the residual geoid heights to remove remaining orbital errors, while CA can be proven a valuable tool to reduce part of the sea surface variability (SSV) that contaminates GM altimetry (Vergos 2002). The present study has a local character, thus a regional crossover adjustment scheme with a bias and a tilt parameter per arc, cf. Knudsen (1992a), is sufficient. The so-derived residual SSHs can be safely regarded as residual geoid heights (N_{res}). The estimation of gravity anomalies from altimetry is performed using the efficient 2D planar FFT inverse Stokes convolution and employing discrete spectra for the kernel function (Schwarz et al. 1990). In all cases 100% zero-padding is appended around the N_{res} to avoid circular convolution effects. It is well known that inverse Stokes is a differentiation, which enhances the high frequencies. Thus, the residual geoid heights have to be low-pass filtered to remove any remaining SSV-like effects, whether else the estimated gravity will be contaminated by noise. The reduction of the SSV is achieved by low-pass filtering the gridded N_{res}, using a collocation type of filter (Wiener filtering). This is performed in the frequency domain by multiplying the geoid spectrum $N(\omega)$ with the filtering function $F(\omega)$ (cf. Eq. 3 in Vergos and Sideris 2002b). The cut-off frequency ω_c is empirically determined based on maximum noise reduction with minimum signal loss. In that filtering operation different cut-off frequencies should be tested to select the one that provides the best Δg_{res}, based on the aforementioned criterion. After the prediction of the residual gravity anomalies the contribution of the geopotential model is restored to estimate the final altimetric gravity field. This procedure is presented in more detail in Vergos and Sideris (2002b) (this issue).

To estimate the SST, altimetric gravity anomalies (Δg^{alt}) are interpolated at the points where shipborne gravity (Δg^{gr}) is available; their difference gives the Δg(QSST). It is important to point out that the shipborne gravity data refer to the geoid too, i.e. free-air gravity anomalies are available with the free-air reduction being estimated as $\delta g_f=-0.3086H$ where H is the QSST from the global model previously used for the correction of the SSHs. Such an approximation for the free-air gradient is sufficient since the SST reaches a maximum of 2.2 m worldwide. The computed $\Delta g(QSST)$ corresponds to the SST spectrum of wavelengths shorter that what the global SST model provides. In the present study the global EGM96 SST model was used, which is complete to degree and order 20 or equivalently represents the SST down to wavelengths of about 2000 km. Consequently, the part of the SST that is estimated with the proposed procedure refers to wavelengths shorter than 2000 km.

After deriving the $\Delta g(QSST)$, and since the shipborne data may contain blunders, a 3 rms test for blunder detection and removal is performed. Then the resulting *residual gravity equivalent SST* is gridded and residual QSST ($\varsigma_{c\ res}$) is estimated using the 1D-FFT spherical Stokes convolution employing discrete spectra for the kernel function. The so-derived residuals represent the SST of wavelengths shorter than 2000 km for the area. At this point we can directly restore the contribution of the global SST and derive the final model. The main problem with this approach is that due to blunders not removed from the data and due to the presence of high-frequency noise, the estimated SST will contain some unexpectedly big or small values.

A way to work out this problem is by filtering the residual SST in order to smooth out and reduce the aforementioned effects. This filtering operation can be performed using different selections of filters, since the spectral content of the noise to be removed is practically unknown. Taking into account that the signal to be modeled is long wavelength in nature, traditional low-pass filtering was selected and different cut-off frequencies were tested. Thus, the collocation type of filter presented in the previous section (cf. Fig. 1 in Vergos and Sideris 2002b) was used to provide the final SST residuals. The disadvantage of low-pass filtering is that ω_c's selection is based on the spectral characteristics of the field only, while its spatial characteristics are not taken into account. Thus, a trial and error process is carried out to determine the *optimal* cut-off frequency. This can be overcome by using a wavelet (WL) transform to detect and smooth irregularities due to the presence of noise or blunders in the estimated SST (see the analysis in paragraph 2.1). After estimating the filtered $\varsigma_{c\ res}$ the contribution of the global model is restored and the final SST model for the area under study is available. The procedure for SST modeling is presented in Fig. 1.

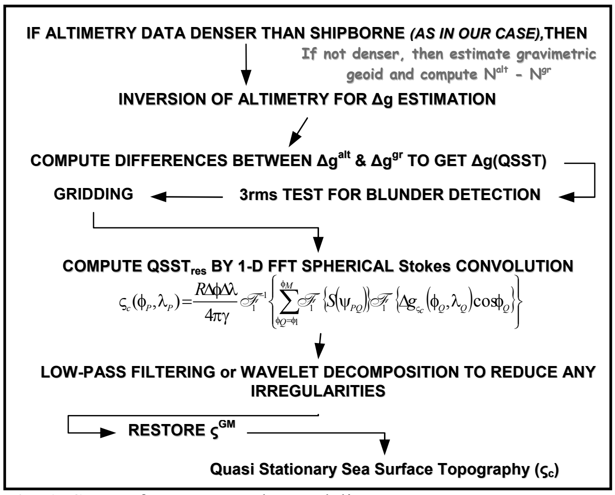

Fig. 1: Sea surface topography modeling.

2.1 Application of wavelets as a multiscale differential operator

To apply wavelets, the frame theory can be used as a generalization of base functions (Christensen 2001). The definition of a frame is

Definition 1: A family of elements $\{\psi_n\} \subseteq H$ (H is a separable Hilbert space) is called frame for H if there exist constants P, $Q > 0$ such that

$$P\|f\|^2 \leq (f, \Psi_n) \leq Q\|f\|^2, \quad f \in H \tag{1}$$

where P,Q are called frame bounds, ψ_n is a family of wavelets and f the signal.

The frame bounds are not unique and the wavelet coefficients in this case are not unique as well. The optimal frame bounds are the biggest possible P and smallest possible value for Q. If we choose $P=Q$ the frame is called tight and when $P=Q=1$ we have an orthonormal basis. From a mathematical point of view the lack of uniqueness is not desirable but the wavelet frames could provide more flexibility in detecting and smoothing irregularities. Because wavelet coefficients are spatially distributed the signal can be smoothed at certain places only and be left unchanged in others. The properties of wavelets to give not only the frequencies of a signal but also their spatial distribution in different scales can be used to detect discrepancies in the data and/or between different sets of data. The approximation coefficients in wavelet decomposition correspond to a low pass filter and detail coefficients are related to the high frequency content of the signal. If all detail coefficients are restricted up to zero, then the wavelet decomposition and reconstruction can be expected to act as a low pass filter. According to the frame theory one can choose the frame bounds and determine corresponding cut off values for the detail coefficients. The choice of this threshold value is important since it will determine the balance between real signal and errors removed.

The spatial distribution of wavelet coefficients allows the use of a wavelet decomposition and reconstruction to smooth data only where irregularities exist. After the decomposition up to a certain level, irregularities can be eliminated in the high frequency part of the decomposition. This is equivalent to putting constraints on the n^{th} derivatives, i.e., smoothness conditions are used. The necessary and sufficient conditions for a wavelet transform to be an n-order multiscale differential operator is the corresponding wavelet to have n vanishing moments (Mallat 1998). It is known that Daubechies wavelets of order N have N-1 vanishing moments. Wavelet decomposition and reconstruction allow the restriction of the vertical, horizontal and diagonal coefficients up to certain level for every level of decomposition. The threshold value is determined as either zero or equal to the RMS value of all detail coefficients for every level of decomposition. These constraints mean that we have implicitly used additional smoothness conditions on the derivatives of the solution. Restricting the detail coefficients on places with great discrepancies means that the horizontal gradients of the signal are forced on both sides of the discrepancies to be equal and to have as values the RMS values for every level of decomposition or be equal to zero. The choice of the threshold value has to be as much as close to the signal-to-noise ratio and needs further investigation. In the present study, two selections for the threshold were made, i.e., one equal to zero and another equal to the RMS value for every level of decomposition. Thus, two WL solutions for the QSST and the geostrophic currents were derived.

3 Geostrophic Velocity Estimation

Having estimated the QSST with the procedure described in the previous section, geostrophic current velocities can be estimated under the assumption of geostrophic flow. This method is more related to oceanographic studies and products, but its main advantage is that it quickly gives velocity estimates and takes into account the properties of the ocean as a fluid. The equations of geostrophic flow in spherical approximation, are given as (Pond and Pickard 2000)

$$u_s = -\frac{g}{fR}\frac{\partial H}{\partial \phi} \tag{2}$$

$$v_s = \frac{g}{fR\cos\phi}\frac{\partial H}{\partial \lambda} \tag{3}$$

where u_s and v_s are the horizontal constituents of geostrophic flow, R is the mean Earth radius, φ and λ

denote geographic latitude and longitude respectively, f is the Coriolis force and H the QSST. Thus, knowing the QSST the geostrophic flow velocities can be determined.

4 Data Used and Area under Study

The area under study is located offshore Newfoundland, Eastern Canada bounded between $40^o \leq \varphi \leq 50^o$ and $310^o \leq \lambda \leq 320^o$. ERS1 and GEOSAT GM satellite altimetry data from the latest releases of their GDR's have been extracted from the databases of AVISO (1998) and NOAA (1997) respectively. The local depth models used to take into account the effect of the bathymetry were those developed by Vergos and Sideris (2002a) using satellite altimetry and depth soundings. Finally, the EGM96 geopotential model, complete to degree and order 360, and the EGM96 DOT, complete to degree and order 20, were used to provide the long wavelength geoid information and the QSST respectively (Lemoine et al. 1998). The shipborne gravity data come from the databases of BGI and the Geodetic Survey Division of Natural Resources Canada comprising of 97474 observations. Since their distribution in the eastern part of the area was sparse ($318^o \leq \lambda \leq 320^o$), they were augmented by the $2' \times 2'$ KMS99 global altimetry-derived gravity field model (Andersen and Knudsen 1998).

5 Sea Surface Topography Estimation

The development of altimetric gravity field models will not be discussed in this paper, since all the intermediate steps and results, together with the validation, are given explicitly in Vergos and Sideris (2002b) (this issue). Two single- and one multi-satellite solutions were developed and the model to be used for the SST estimation was selected upon its agreement with shipborne gravimetry. The altimetric gravity model finally selected was the one from GEOSAT (see Table 1), which gave also the best agreement with KMS01 at the ±4.9 mGal level (1σ). From Fig. 2, where the comparison between the GEOSAT solution and shipborne gravity is depicted, it is evident that the differences are small throughout the region and present some big values in the south-west part only. These differences have a track-like pattern and follow a few shipborne tracks from the BGI database; we can thus conclude that they are due to blunders in the ship data. To remove these blunders a 3 rms test is performed with the results presented in Table 2, where the elimination of part of these blunders can be seen.

Table 1. Differences between shipborne gravimetry and the estimated models. Unit: [mGal].

	max	min	mean	σ
$\Delta g^{ship} - \Delta g^{GEOSAT}$	120.2	-79.2	-0.1	±15.5
$\Delta g^{ship} - \Delta g^{ERS1}$	118.9	-88.8	-0.1	±16.5
$\Delta g^{ship} - \Delta g^{combined}$	120.0	-83.4	0.0	±15.9
$\Delta g^{ship} - \Delta g^{KMS01}$	118.5	-82.6	0.1	±15.6

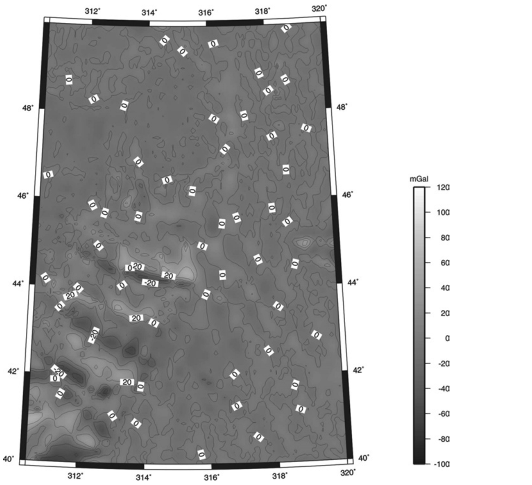

Fig. 2: Gravity anomaly differences between shipborne gravimetry and the GEOSAT solution.

Table 2. Gravity equivalent QSST before and after the 3 rms test. Unit: [mGal].

	max	min	mean	σ
Δg(QSST) (before)	79.0	-119.5	0.1	±15.6
Δg(QSST) (after)	43.1	-42.1	-0.3	±13.8

After that step the residual field was gridded using a 3′ grid spacing and a weighted means with prediction power two type of interpolation, so that residual QSST could be predicted using the 1D-FFT. Table 3 (first two rows) presents the estimated $\varsigma_{c\ res}$ where it is evident that QSST of wavelengths shorter than 2000 km can be estimated. The quite high and low max and min values, are noticing and signal the effect of noise and blunders still present in the residual field. The statistics of the final SST model, after restoring the contribution of the global EGM96 model, are presented in Table 3, where it is seen again that the SST model reaches a min value of about -1.5 m which can be regarded as too low for the region. Additionally, from Fig. 3 the effect of the blunders in the ship data is evident in the final model (SW part of the area). Nevertheless, in the rest of the region the estimated SST follows very well the bathymetry and depicts the general flow of some big currents such as the Labrador Current around the Newfoundland Grand Banks.

Table 3. Statistics of residual and final QSST from the original and low-pass filtered solutions. Unit: [m].

	max	min	mean	σ
$\varsigma_{c\ res}$ **(original)**	0.99	-1.14	0.10	±0.26
ς_c **(original)**	0.94	-1.47	-0.28	±0.32
$\varsigma_{c\ res}$ **(LP filtered)**	0.54	-0.76	0.00	±0.22
ς_c **(LP filtered)**	0.35	-1.11	-0.38	±0.28

The estimated current velocities range from -5 to 5.6 m/s, while normally, based on the circulation of the area, they should reach values up to 2 m/s. That is clear from Fig. 4 (left), where the estimated velocity vector field is depicted. It is obvious that even though we manage to depict the main currents in the area, the presence of blunders and noise in the final estimates in the southwest part of the region is dominant.

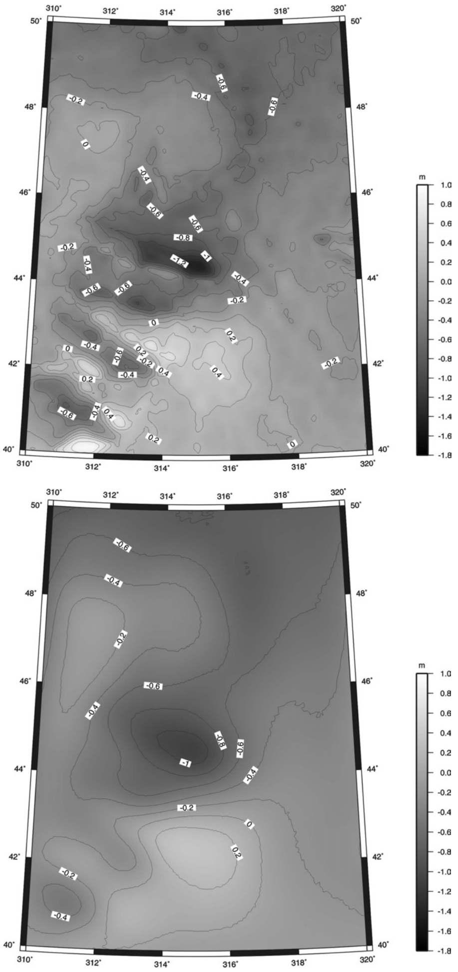

Fig. 3: The final estimated QSST models based on the original (top) and low-pass filtered solutions (bottom).

Table 4. Geostrophic velocities from the original and low-pass filtered solutions. Unit: [m/s].

	max	min	mean	σ
u_s (original)	5.61	-3.51	0.07	±0.65
v_s (original)	4.11	-5.08	0.01	±0.52
u_s (LP filtered)	-0.71	-1.15	0.06	±0.22
v_s (LP filtered)	0.51	-0.78	-0.01	±0.21

To eliminate such effects, the residual QSST estimates were low-pass filtered using the aforementioned Wiener-type of filter and a cut-off frequency equivalent to 100 km wavelength. Tables 3 and 4 (last two rows in each) present the statistics of the residual and final SST model and the geostrophic velocities, respectively. It can be easily seen that by filtering the data, a smoother field is estimated and the final QSST varies within an expected range. The same, as in the original solution, patterns in the QSST model are depicted (see Fig. 3) but now both the noisy features and the blunders in the central/southwest part of the area are removed. The estimated geostrophic velocities range between -1.1 to 0.5 m/s and manage to represent clearly the circulation pattern of the area (see Fig. 4), i.e. two branches of the Labrador Current (LC), a branch of the Gulf Stream (GS), a strong stream (1) with an east-west direction, an anticyclone (2) and a cyclone (5), a branch of stream (1) going northwards around Flemish Cap (3) and finally a number of smaller in velocity streams (4) merging onto GS. This is a good indication that by LP filtering the estimated $\varsigma_{c\ res}$ we manage to estimate a better model of the QSST of the area and represent far more realistically the oceanic circulation.

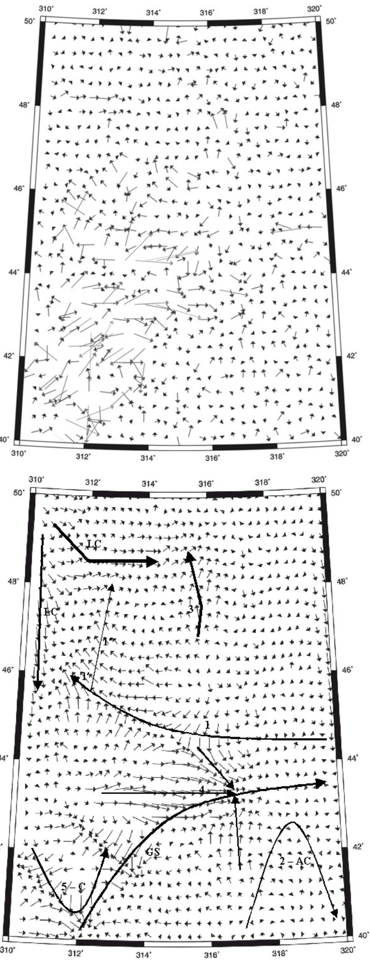

Fig. 4: The estimated current velocity vector fields based on the original (top) and low-pass filtered solutions (bottom).

Finally, the experiments with the WL transform were performed and two solutions were estimated, i.e. one by setting all detail coefficients for every level of decomposition to zero (WL_zero) and another by setting them to the RMS value (WL_rms). Going up to the 5th level of decomposition, corresponding to a resolution of 96 km, was sufficient to smooth the irregularities in the estimated QSST. Table 5 presents the statistics of the two estimated QSST models based on the aforementioned approaches. As expected, the WL_zero solution is very close to the one from LP filtering since by setting all detail coefficients to zero we perform something similar to low-pass filtering. The difference between the LPF and WL_zero solutions is at the ±5 cm (1σ) only signaling the equivalence of the two methods. Their difference lies to the localization property of wavelets, which enables the detection and further, compared to LPF, smoothing of the irregularities in the $\varsigma_{c\ res}$. The

WL_rms solution gives results close to the ones from the original data, i.e. high values for both the QSST and the velocities of the currents. This is an indication that the rms value is not a proper selection to smooth the irregularities in the data. We acknowledge the fact that setting the detail coefficients equal to zero is arbitrary too and that further research has to be directed to that field based on the spatial and spectral properties of the signal (QSST) that have to be retained and those that have to be removed. Nevertheless, the good results and the agreement between the LPF and WL_zero solutions provide a good validation for both approaches.

Table 5. Statistics of the final QSST using WL transform. Unit: [m].

	max	min	mean	σ
ς_c (WL_zero)	0.47	-0.99	-0.28	±0.29
ς_c (WL_rms)	0.67	-1.41	-0.28	±0.31

6 Conclusions and Future Research

Satellite altimetry and shipborne gravity data have been used in the present study to estimate the quasi-stationary sea surface topography and velocities of the geostrophic currents. Both the determination of gravity anomalies from satellite altimetry and the subsequent estimation of the final residual sea surface topography are based on the efficient 1D ad 2D FFT. Low-pass filtering and wavelet transform have been used to smooth out irregularities, due to noise and blunders, present in the data aiming to derive better estimates of both the QSST and the geostrophic velocities.

The results of the experiments performed show that, based on the proposed methodology, it is possible to estimate QSST of wavelengths shorter than about 2000 km. But, it is necessary to perform some kind of smoothing (filtering) to the estimated residual QSST field so that the effect of high-frequency noise and blunders in the data will be removed or at least reduced. This leads to more realistic, at least for the area under study, SST and associated current velocity estimates.

When using the collocation type of filter we manage to depict the main currents, streams and gyres in the area, while smaller in magnitude features, such as an anti-cyclone and a cyclone are identified as well. The wavelet transform seems to be a valuable tool for the detection and smoothing of irregularities in the data, while it is shown that by setting the detail coefficients to zero rather than the rms value gives superior results.

The presented results demonstrate the usefulness of geodetic methods in the determination of oceanographic quantities and prove the importance of the interaction between these two sciences. Our future work will be directed to the spectral analysis of the estimated $\varsigma_{c\ res}$ to verify the existence of short-wavelength QSST, the selection of an optimal value for the restriction of the detail coefficients in the wavelet solutions and the comparison of the estimated QSST with oceanographic models.

Acknowledgements

This research was performed while the first author was a graduate student at the University of Calgary. Financial assistance, provided by NSERC and the GEOIDE Network of Centers of Excellence is gratefully acknowledged. BGI and Mr. Marc Véronneau from GSD/NRCan are gratefully acknowledged for providing the shipborne gravity data. We would like to thank Dr. Martin Vermeer and an anonymous reviewer for their constructive comments on an earlier version of the paper.

References

Andersen OB, Knudsen P (1998) Global gravity field from ERS1 and Geosat geodetic mission altimetry. J Geophys Res 103(C4): 8129-8137.

AVISO User Handbook – Corrected Sea Surface Heights (CORSSHs). AVI-NT-011-311-CN, Edition 3.1, 1998.

Christensen O (2001) Frames, Riesz bases and discrete Gabor/Wavelet expansions, Bulletin of the American Mathematical Society, Volume 38, Number 3, 273-291.

Engelis T (1983) Analysis of sea surface topography determination using Seasat altimeter data. Report No. 343, Department of Geodetic Science and Surveying, The Ohio State University, Columbus, Ohio.

Engelis T (1985) Global circulation from Seasat altimeter data. Marine Geodesy, Vol. 9, No. 1.

Engelis T (1987) Spherical harmonics expansion of the Levitus sea surface topography. Report No. 385, Department of Geodetic Science and Surveying, The Ohio State University, Columbus, Ohio.

Knudsen P (1992a) Altimetry for Geodesy and Oceanography. In Geodesy and Geophysics, Kakkuri J (ed), pp. 87-129. Finnish Geodetic Institute.

Knudsen (1992b) Estimation of sea surface topography in the Norwegian sea using gravimetry and Geosat altimetry. Bulletin Géodésique 66:27-40.

Lemoine FG, Kenyon SC, Factor JK, Trimmer RG, Pavlis NK, Chinn DS, Cox C, Klosko SM, Luthcke SB, Torrence MH, Wang YM, Williamson RG, Pavlis EC, Rapp RH, Olson TR (1998) The development of the join NASA GSFC and NIMA geopotential model EGM96, NASA Technical Paper, 1998 – 206861.

Mallat S (1998). A wavelet tour of signal processing. Academic Press, USA.

National Oceanographic and Atmospheric Administration – NOAA (1997) The GEOSAT-GM Altimeter JGM-3 GDRs.

Pavlis NK, Cox CM, Wang YM, Lemoine FG (1998) Further analysis towards the introduction of ocean circulation model information into geopotential solutions. Boll Geof Teor Appl, Vol 40(3-4), pp 359-369.

Pond S, Pickard G (2000) Introductory dynamical oceanography. 2nd edition, Butterworth – Heinemann.

Schwarz KP, Sideris MG, Forsberg R (1990) The use of FFT techniques in physical geodesy. Geophys J Int 100:485-514.

Vergos GS (2002) Sea Surface Topography, Bathymetry and Marine Gravity Field Modelling. MSc Theses Dissertation, Dept of Geomatics Engineering, University of Calgary, UCGE Reports 20157, Calgary, Alberta, Canada.

Vergos GS, Sideris MG (2002a) Improving the Estimation of Bottom Ocean Topography with Altimetry-Derived Gravity Data Using the Integrated Inverse Method. International Association of Geodesy Symposia, Vol. 124 Ádam J Schwarz KP (eds.), *Vistas for Geodesy in the New Millennium*, Springer – Verlag Berlin Heidelberg, pp. 529-534.

Vergos GS, Sideris MG (2002b) Altimetry-Derived Marine Gravity Field Estimation Using Single- and Multi-Satellite Data. Presented at the 3rd Meeting of the IGGC, Thessaloniki, Greece, August 26-30.